Axial and low-symmetry centers of trivalent impurities in lithium niobate: Chromium in congruent and stoichiometric crystals

G. Malovichko* and V. Grachev
Department of Physics, University of Osnabrueck, D-49069, Osnabrueck, Germany
and Institute for Problems of Material Sciences, National Academy of Sciences of Ukraine, Kiev, Ukraine

E. Kokanyan
Institute for Physical Researches, Ashtarak, Armenia

O. Schirmer
Department of Physics, University of Osnabrueck, D-49069, Osnabrueck, Germany
(Received 1 September 1998)

A systematic analysis and classification of clusters, consisting of impurity (extrinsic) and intrinsic defects in lithium niobate crystals, were made in order to understand the main features of the observed EPR spectra. It is shown that possible configurations for lithium substitution with charge compensators such as a lithium vacancy (X_{Li}-Y_{Li}), niobium vacancy (X_{Li}-Y_{Nb}), and oxygen interstitial ions (X_{Li}-Y_i) belong to C_3 or C_1 point group symmetries; this is also valid for the complexes with niobium substitution and the $\mathrm{Nb_{Li}}$ antisite as the compensator (X_{Nb}-Y_{Li}). Clusters of an oxygen vacancy and an impurity on a niobium site (X_{Nb}-Y_{O} configurations) have C_1 symmetry only, but never C_3 symmetry. A detailed study of EPR spectra for a wide set of crystals with different chromium concentrations and [Li]/[Nb] ratios was carried out. Besides the main axial Cr^{3+} center, eight satellite chromium centers were experimentally resolved and parameters of their spin Hamiltonians were determined by fitting angular dependences of EPR lines. It was found that in stoichiometric material less chromium is incorporated into the crystal and that the satellite centers disappeared. A correlation of EPR, optical absorption, and luminescence spectra was observed and analyzed. The existence of the family of chromium centers was explained on the basis of one common hypothesis about charge compensation by intrinsic defects. In a minimal model, sufficient to explain all experimental data, it is assumed that the satellite centers include two defects — $\mathrm{Cr_{Li}}$ and niobium vacancy v_{Nb} in the first or further neighboring shells. Two v_{Nb}'s compensate five $\mathrm{Cr_{Li}}$. Since in conventional congruent crystals the relative concentration of additional satellite centers is comparable with the concentration of the main center, the conclusion was made that both kinds of centers are equally responsible for many of the lithium niobate properties. [S0163-1829(99)08613-0]

Trivalent ions, including those of transition metals and rare-earth elements, belong to the most important impurities in lithium niobate (LN, $LiNbO_3$) because of their essential influence on properties of this material (such as domain structure, electro-optical coefficients, light absorption, refractive indices, etc.) and their consequences for present and potential applications. Especially the investigation of Cr^{3+} centers in LN has a long history and the number of publications devoted to the spectroscopic studies of such defects in LN already surpasses some dozens. With the first optical and EPR studies of Cr^{3+},[1–4] mainly a discussion about the location of the Cr^{3+} impurity in the crystal lattice was opened. A lot of effort was also spent to establish a correlation between the observable spectra and the crystal composition and to develop experimentally supported models of the Cr^{3+} centers. Nevertheless the structure of even the main centers (such as the position of the Cr^{3+} ions in the lattice, their nearest surroundings, the way of charge compensation) has not yet been determined definitely.

In the course of the investigation of such defect structures in LN one meets the following difficulties:

(i) High-quality conventional crystals are usually grown from the congruent melt with $x_m = x_C \approx 48.4\%$ ($x = [\mathrm{Li}]/([\mathrm{Li}]+[\mathrm{Nb}])$); this means that the congruent crystals contain many intrinsic (nonstoichiometric) defects, causing a broadening of the observable spectral lines and ambiguities in their interpretation;

(ii) The crystal composition x_C of the undoped LN depends on the melt composition x_m and the growth conditions; only for the congruent composition $x_m = x_C$;

(iii) The most probable positions for impurity incorporation, the Li and Nb sites as well as the structural vacancy, have the same local symmetry C_3; this means that they are not distinguishable by many spectroscopic techniques including EPR;

(iv) Defects at other sites or complexes of two defects, if they are not extending along the crystal axis, have the lowest C_1 point group symmetry.

The following five models were proposed in literature for the Cr^{3+} centers in $LiNbO_3$: (1) indefinite sites with C_3 symmetry for the main center;[1,4–6] (2) Nb substitution;[2,3,7–13] (3) Li substitution;[14–22] (4) different sites for different observable centers;[14,19,23–28] (5) Li^+ and Nb^{5+} replaced by $Cr^{3+}+Cr^{3+}$.[15,29–38]

Most of these investigations were devoted to the main axial Cr^{3+} centers (point-group symmetry C_3). In some of the articles it was also pointed out that there are additional lines in the spectra of EPR,[4,14,19,23–25,29] optical absorption,[21,33,34,37,38] and luminescence[19,26,28,30,33,34,36] of conventional LN. Taking into account the difficulties described above, the available restricted growth and research opportunities for many authors (especially in the early years), the hard work and persistence of the researchers in the subtle search of even minor arguments and support for the proposed models should be highly appreciated, however, still some of old and recent experimental facts were not interpreted satisfactorily so far and none of the models can be accepted unconditionally.

Recently, several ways to obtain stoichiometric LN crystals (i.e., with $x_C \approx 50\%$) were developed: (a) vapor transport equilibration treatment of initially congruent crystals in Li-excess powder of LN;[39] (b) the double crucible method in which crystals are pulled from the melt with fixed Li concentration;[40] (c) crystal growth from the melt, to which K_2O has been added.[41–43]

Independently of the method of production, such stoichiometric LN is a very attractive material for the study of physical properties of LN because of several reasons. First of all this is a material whose characteristics are not masked by the presence of intrinsic defects. The second, a tremendous (up to 10 times) narrowing of spectral signals, measured by various techniques, essentially increases their resolution and thus allows us to obtain more detailed information than in the case of congruent crystals. The third, new centers and features appear as a consequence of the refinement of the material from nonstoichiometric defects.

It should be noted that formerly in some articles the term ''stoichiometric LN'' was often associated with samples grown from a stoichiometric melt ($x_m = 50\%$, resulting in x_C about 48.9% only). During recent years the term is used instead mainly for crystals with the composition really close to $x_C \approx 50.0 \pm 0.1\%$.

The first part of this article consists of a general analysis of possible centers, which can be produced by trivalent impurities Me^{3+} in ideal and conventional LN. The second part is devoted to the detailed study of chromium centers in LN crystals with different x_C and Cr content, and to the discussion and determination of the models, which are able to explain all experimental data for these centers. The main results presented here are obtained with the help of EPR. A comparison with the conclusions based on other methods [optical absorption, luminescence, electron-nuclear double resonance (ENDOR) etc.] is also given in order to reach a consistent interpretation of the features of the investigated crystals. Possible reasons, why diverging conclusions of other authors differ from the present ones, are discussed briefly.

CRYSTALS, EQUIPMENT, COMPUTER PROGRAMS

A special series of samples, grown by the Czochralski method from the melts with different chromium concentrations (0.002–1.08 wt. %) and different x_m ratios (43–60 %) were used. One further set of crystals with different chromium contents was grown from a congruent melt with the addition of K_2O under special conditions, leading to stoichiometric or nearly stoichiometric samples. Identical starting materials (Li_2CO_3, Nb_2O_5, and K_2CO_3) from one source were used for the growth of all these crystal series. Several undoped and chromium-doped crystals from different other sources were also studied for comparison. This systematic approach, intentionally varying the composition of the crystals and their impurity content, allowed us to obtain spectra representing the common properties of LN and the tendencies of their changes, but not features of accidental samples with unknown noncontrolled impurities.

The actual crystal compositions x_C were determined by the analysis of the EPR and NMR line widths and the intensity ratios of the forbidden and allowed resonance transitions.[42–44] It was found that crystals grown from melts with x_m equal to 43.0, 48.5, 54.5, and 60.0 % have compositions x_C approximately equal to 47.0, 48.5, 49.5, and 49.85 %. Crystals pulled from melts containing K_2O possess an x_C of about 50.0%.

Most of the EPR and some ENDOR measurements were carried out in the temperature range 4.2–300 K at the *X* band on a Bruker ESR-200 D-SRC with the ESP 360 DICE ENDOR system at the University of Osnabrück. Besides that *Q*- and *X*-band EPR investigation in the range 77–300 K were fulfilled by means of RE-1301, RE-1308 spectrometers at Kiev. Optical absorption spectra were measured using a Bruins Instruments Omega 10/20 spectrometer.

The wealth of information contained in the spectra and their very involved angular dependences could only be exploited using advanced numerical methods for their treatment (filtering, peak picking, simulations, spectra subtraction, etc.). For this purpose the VISUAL EPR program package[45] was used. The determination of the relevant spin-Hamiltonian parameters of paramagnetic centers was made by a fitting procedure, based on exact diagonalization of the corresponding matrices.

LN LATTICE AND POSSIBLE STRUCTURES OF IMPURITY CENTERS

The ideal LN lattice (Fig. 1) has two $LiNbO_3$ molecules in its rhombohedral elementary unit cell and the space-group symmetry is $R3c$ at room temperature.[46–50] There are several electrically nonequivalent positions in the lattice. Some of them — the sites on the **z** (or optical **c**) axis of the crystal, including the sites of Li, Nb and the structural vacancy, v — have the symmetry of the point group C_3. An isolated defect in any of these positions creates a C_3 (in the following also labeled ''axial'') center. All other positions have the lowest possible symmetry, C_1. A complex of two defects has C_3 symmetry, if both are located on the crystal **z** axis, and C_1 symmetry in all other cases. If the difference in positions of the nearest oxygen ions is ignored, then each unit cell has the following site sequence along the **z** axis: Li, Nb, v_{oct}, Li, Nb, v_{oct}. However, oxygen octahedra and next neighbors for two positions of one type cation are not identical, therefore the correct assignment of the sequence should be Li_L, Nb_L, $v_{\mathrm{oct},L}$, Li_R, Nb_R, $v_{\mathrm{oct},R}$. The surroundings of the right (R) positions can be transformed to the left (L) ones by a reflection $\mathbf{x} \leftrightarrow -\mathbf{x}$ and a shift by $c/2$, because **zy** is a glide mirror plane in the $R3c$ lattice. The same consideration is applicable to C_1 positions also. This means that each axial (C_3)

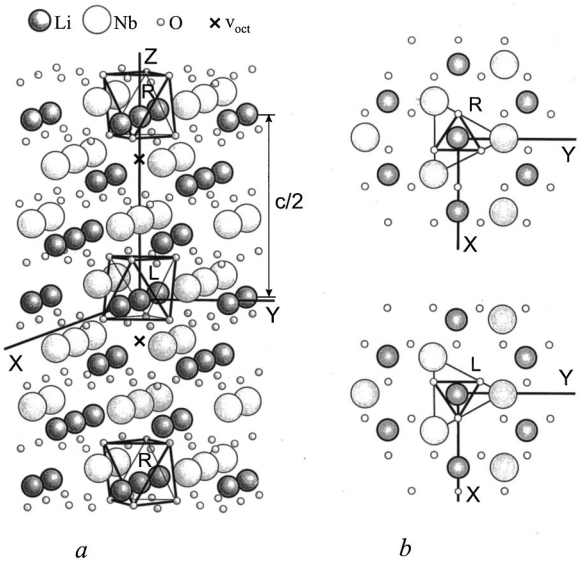

FIG. 1. (a) ideal lattice of lithium niobate. To simplify the representation of the lattice and defect structures in it, the sizes of ''balls'' imitating ions were made intentionally different. If real ionic radii are taken into account (Li^+-0.68 Å, Nb^{5+}-0.69 Å, O^{2-}-1.32 Å), the LN lattice looks like it consists mainly of planar layers of closely packed oxygen ions with small voids between them, filled by Li and Nb. Left and right positions are distinguished by their different oxygen surroundings. (b) illustration of local C_3 symmetry for the nearest surroundings of cation sites. A projection of three Li, Nb, and O layers on the **xy** plane is shown.

or low-symmetry (C_1) L center has a corresponding R partner. The L and R partners are electrically identical and are not distinguishable by optical methods, but they are magnetically nonequivalent and can be resolved from each other in favorable cases (high spin value, small linewidth) by magnetic resonance techniques.

The usual spin-Hamiltonian, which describes the field positions of the EPR lines of the centers with C_1 symmetry, can be written as

$$H=\beta\mathbf{BgS}+\Sigma_{kq}(b_k^qO_k^q+c_k^q\Omega_k^q),\quad k\leqslant 2S+1,-k\leqslant q\leqslant k. \quad (1)$$

Here β is the Bohr magneton, **B** is the vector of static magnetic field, **g** is the g tensor, S is the total electron spin of paramagnetic center, b_k^q,c_k^q are parameters of crystal field, O_k^q,Ω_k^q are irreducible tensor operators of electron spin, which are defined in Ref. 51. For C_3 symmetry the spin-Hamiltonian has only crystal-field terms with $q=0,3,6$ and diagonal components of the g tensor.

All parameters of the spin-Hamiltonian for L and R centers have the same absolute values, but $g_{xy}(L)=-g_{xy}(R)$, $g_{zx}(L)=-g_{zx}(R)$, $b_k^q(L)=-b_k^q(R)$ for $q=1,3,5$ and $c_k^q(L)=-c_k^q(R)$ for $q=2,4,6$. This leads to a splitting of the resonance lines of the L and R centers, if the magnetic field deviates from the **z** axis in the **zx** plane. For $S\geqslant 2$ even lines of C_3 centers are split because of the existence of the $b_4^3O_4^3$ term in crystal field: $b_4^3(L)=-b_4^3(R)$. When **B** is rotated around the **x** axis (i.e., in the **zy** plane), the lines of both centers always coincide, however some asymmetry of the angular dependencies with respect to the change of the polar angle θ to $180°-\theta$ can be observed.

In the $R3c$ lattice each C_1 center has two additional magnetically nonequivalent partners, which can be transformed into each other by a rotation around the **z** axis of the crystal by 120° and 240°. Therefore at arbitrary orientations of the magnetic field each of the resonance transitions can produce one (for $S<2$) or two (for $S\geqslant 2$) lines for C_3 centers and six lines for low-symmetry centers (for any spin value).

Because of nonstoichiometry the real lattice of conventional LN contains many intrinsic defects, the nature of which has not yet been reliably determined. The following entities have been considered (their charges with respect to the lattice being given by Kröger-Vink notation in brackets): $Nb_{Li^+}^{5+}(Nb_{Li}^{4*})$ antisite defect, $v_{Li}^{+}(v'_{Li})$ lithium vacancy, $v_{Nb}^{5+}(v_{Nb}^{5'})$ niobium vacancy, $Nb_v^{5+}(Nb_v^{5*})$ niobium on structural vacancy, $Li_v^+(Li_v^*)$ lithium on structural vacancy. During recent years the existence of the following charge compensated complexes has been postulated most often: $Nb_{Li}+4v_{Li}$,[48,52,53] $5Nb_{Li}+4v_{Nb}$,[54,55] $2Nb_{Li}+2Nb_v+3v_{Li}+3v_{Nb}$.[56] The intrinsic defects by themselves or complexes of them, which are not charge compensated, can furthermore serve as local or distant charge compensators for nonisocharged substitutional or interstitial impurities.

Angular dependences of a center without any other defect in its nearest neighborhood (distant charge compensation) correspond to the symmetry of the occupied site, i.e., C_3 for the sites on the **z** axis and C_1 for all other cases. However, the presence of distant defects can reveal itself by a specific broadening of the EPR lines and an asymmetry of their shape.

The structure of a center, in which a lattice site is occupied by an extrinsic impurity ion having a charge different from that of the respective lattice site (in the following labeled nonisocharged replacement) depends on the charge of the impurity and the mechanism of charge compensation. Below the trivalent state Me^{3+} is considered in detail, because many transition metals (including iron and chromium) and rare-earth elements enter LN in this valence.

If Me^{3+} substitutes Li^+ or is incorporated in a structural vacancy, the positive charge excess can be compensated by both v_{Li}^+ and v_{Nb}^{5+} (because Li and Nb vacancies have negative charges with respect to the ideal lattice). For instance every impurity ion at a Li site can be compensated by two lithium vacancies or every five $Me_{Li^+}^{3+}$ ions by two niobium vacancies.

The positive antisite defect Nb_{Li} can serve as a charge compensator for Me^{3+} replacing Nb^{5+} (but not $Me_{Li^+}^{3+}$ or Me_v^{3+}). It is remarkable that one $Nb_{Li^+}^{5+}$ exactly compensates the excess charge of two $Me_{Nb^{5+}}^{3+}$ ions.

The association of $Me_{Li^+}^{3+}$ with v_{Nb}^{5+} in the nearest Nb shell (partial local charge compensation) leads to an axial center, in the second and third Nb shell, to two different C_1 centers, in the fourth Nb shell, to a second axial center, in the fifth to ninth Nb shells, to further five C_1 centers (X_{Li}-Y_{Nb} configurations, Fig. 2; distances between the replaced ion and these shells and the symmetries of the corresponding complexes are given in Table I). A niobium vacancy in the nearest neighborhood disturbs the Me^{3+} surroundings much stronger than distant v_{Nb}. The distance between Me^{3+} and a defect in the fifth to ninth shells is about 6 Å, however a defect as

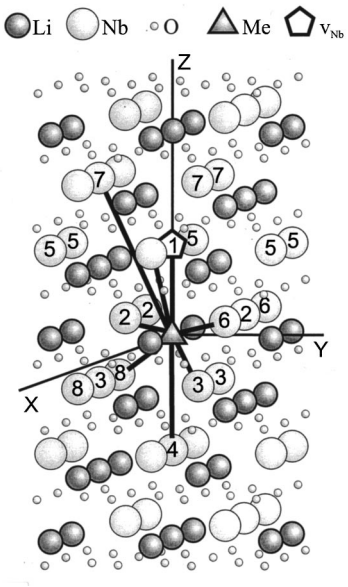

FIG. 2. Possible configurations of X_{Li}-Y_{Nb} (e.g., Me_{Li}-v_{Nb}) defects. The digits 1–8 correspond to the number of niobium shells around the lithium site.

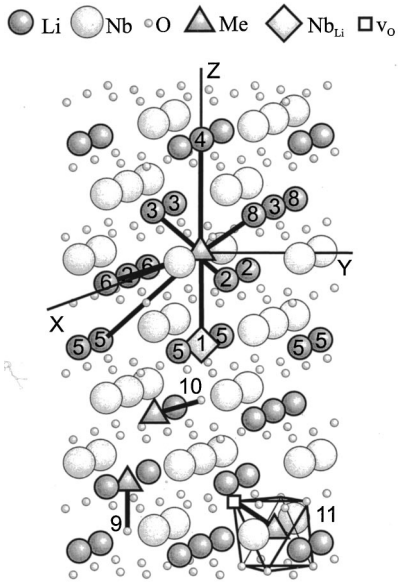

FIG. 3. Possible configurations of X_{Nb}-Y_{Li} (e.g., $Me^{3+}_{Nb^{5+}}$-$Nb^{5+}_{Li^+}$) defects. 1–8 are the number of lithium shells around the niobium site. 9, 10 are the interstitial oxygen (X_{Li}-Y_i or $Me^{3+}_{Li^+}$-O_i^{2-}); 11 is the oxygen vacancy (X_{Nb}-Y_O or $Me^{3+}_{Nb^{5+}}$-v_O^{2-}).

strongly charged as v_{Nb} is still expected to influence the crystal-field parameters even for such a large distance.

The point-group symmetries and distances for the $Me^{3+}_{Nb^{5+}}$-$Nb^{5+}_{Li^+}$ centers have to be similar to those described above, because these defects are located again at the same Nb and Li positions (X_{Nb}-Y_{Li} configurations, Fig. 3, Table I).

In the case of $Me^{3+}_{Li^+}$ compensated by two v^+_{Li} three lattice defects are combined and all partners occupy Li sites only (X_{Li}-Y_{Li} and Y^1_{Li}-X_{Li}-Y^2_{Li} configurations, Fig. 4). Taking into account that differences in the relative locations of the impurity and vacancies can give electrically nonequivalent centers, four distinguishable C_1 configurations can be constructed with two v^+_{Li} in the first Li shell of $Me^{3+}_{Li^+}$ (6 possible sites). One v^+_{Li} in the first shell and one v^+_{Li} in the second shell (also six sites) give 12 electrically nonidentical low-symmetry centers. If one of the lithium vacancies is very far, the presence of only one vacancy in the first shell of $Me^{3+}_{Li^+}$ gives two electrically different configurations, in the second shell, two further ones. Two nearest Li positions on the C_3 axis are located at 6.93 Å and the following, the third one at 13.86 Å. The presence of lithium vacancies on these sites near $Me^{3+}_{Li^+}$ does not break the C_3 symmetry and should generate axial centers only. However, since v^+_{Li} has only one negative charge relative to the ideal lattice, it produces a 4–5 times weaker perturbation of the crystal field than $Nb^{5+}_{Li^+}$ or v^{5+}_{Nb}. Therefore, the centers with v^+_{Li} at distances of about 6 Å should probably not be distinguishable from axial centers with nonlocal charge compensation.

TABLE I. Distances between cations in lithium niobate.

Li shells around Nb or Nb shells around Li			Li shells around Li or Nb shells around Nb		
Shell No.	Point group symmetry	Distance Å	Shell No.	Point group symmetry	Distance Å
1	$\mathbf{C}_3$	3.01	1	$\mathbf{C}_1$	3.76
2	$\mathbf{C}_1$	3.05	2	$\mathbf{C}_1$	5.15
3	$\mathbf{C}_1$	3.38	3	$\mathbf{C}_1$	5.49
4	$\mathbf{C}_3$	3.92	4	$\mathbf{C}_1$	6.38
5	$\mathbf{C}_1$	5.96	5	$\mathbf{C}_3$	6.93
6	$\mathbf{C}_1$	5.99	6	$\mathbf{C}_1$	7.53
7	$\mathbf{C}_1$	6.09	7	$\mathbf{C}_1$	8.20
8	$\mathbf{C}_1$	6.16	8	$\mathbf{C}_1$	8.63
9	$\mathbf{C}_1$	6.47	9	$\mathbf{C}_1$	8.92
10	$\mathbf{C}_1$	6.90	10	$\mathbf{C}_1$	9.12

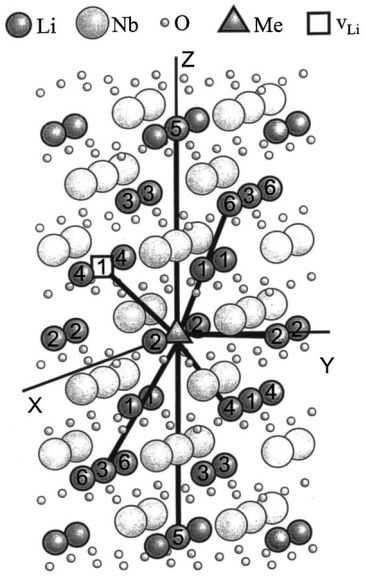

FIG. 4. A part of possible X_{Li}-Y_{Li} (Me_{Li}-v_{Li}) complexes in LN.

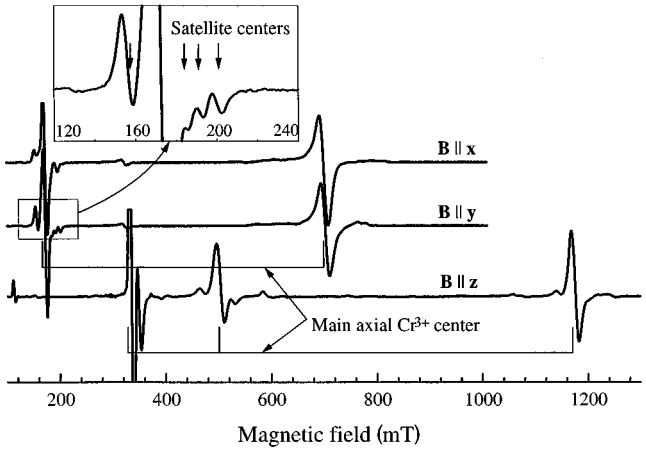

FIG. 5. EPR spectra of Cr^{3+} in LN for $\mathbf{B}\|\mathbf{z},\mathbf{B}\|\mathbf{x},\mathbf{B}\|\mathbf{y}$. Microwave frequency $\upsilon = 9.4$ GHz (X band), temperature $T = 4.2$ K, crystal composition $x_C = 49.85\%$, chromium concentration [Cr] $= 0.02$ wt. %.

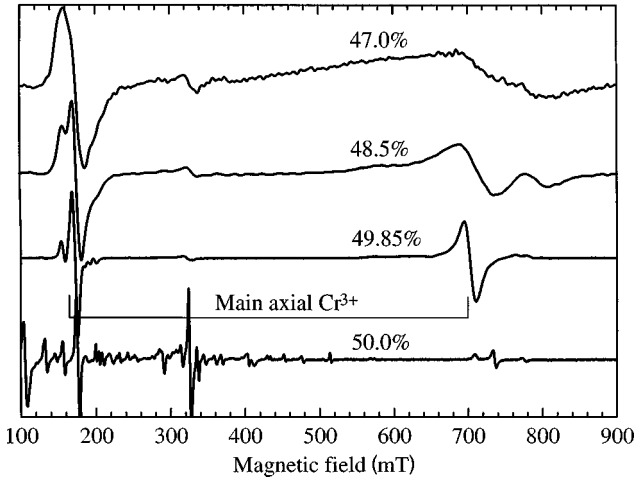

FIG. 6. Dependence of Cr^{3+} EPR spectra on crystal composition x_C. $\mathbf{B}\|\mathbf{y}$, [Cr]$=0.02$ wt. %, $T = 4.2$ K.

Conceivable complexes of $Me^{3+}_{Nb^{5+}}$ and a divalent oxygen vacancy, $\upsilon_{O^{2-}}$, (or other defects in the oxygen sublattice, i.e., X_{Nb}-Y_O configurations) have C_1 symmetry only, but never C_3 symmetry. Oxygen interstitial ions, if present, can compensate only $Me^{3+}_{Li^+}$ and, depending on their relative mutual locations (X_{Li}-Y_i configurations), could give C_3 and C_1 centers (Fig. 3).

To complete the enumeration of potential defect clusters, possible interstitial positions of the trivalent impurities in octahedral or tetrahedral structural vacancies, Me^{3+}_{υ}, should also be considered. In both cases an excess charge can be compensated by υ_{Li} (Me^{3+}_{υ}-$3\upsilon_{Li}$), υ_{Nb} ($5Me^{3+}$-$3\upsilon_{Nb}$), or by interstitial oxygen ions ($2Me^{3+}$-$3O^{2-}_i$), but not by oxygen vacancies or Nb_{Li} antisites. The tetrahedral vacancy site has C_1 point-group symmetry, therefore all centers based on its occupation have this lowest symmetry.

The knowledge of these features helps to identify EPR lines of different centers, if they are simultaneously present in the same sample, and to determine their point-group symmetry and possible structures.

DEPENDENCE OF EPR SPECTRA ON CRYSTAL COMPOSITION x_C AND CHROMIUM CONCENTRATION

EPR spectra of LN:Cr (Fig. 5) look at first sight like rather simple. They consist of three strong lines at $\mathbf{B}\|\mathbf{z}$ and two lines at $\mathbf{B}\|\mathbf{x}$ or $\mathbf{B}\|\mathbf{y}$. Since the positions of the main lines are not changed under rotation of the magnetic field from $\mathbf{B}\|\mathbf{x}$ to $\mathbf{B}\|\mathbf{y}$, they belong to an axial center. This main center was investigated and described earlier (see, for example, Refs. 1, 2, 4, 14) and it was shown that Cr^{3+} with $S = 3/2$ is responsible for these lines. However, if we look carefully on the shape of the lines in Fig. 5, we can see that even for this LN crystal with a rather high crystal composition of $x_C = 49.85\%$ and correspondingly with a low concentration of intrinsic defects the lines are still asymmetric, as well as inhomogeneous, and other additional lines can be seen near and under the main rather broad lines. Such asymmetry and broadening of EPR lines can much more obviously be seen in the spectra of congruent LN:Cr crystals. These details were not completely reproducible in some of previous publications and were very often ignored.

And this is no wonder, since LN is a crystal whose properties depend on many parameters: melt composition, crystal-growth conditions, presence of some background impurities (for example, vanishingly small concentrations of Fe lead to observable changes of the crystal composition and its characteristics[44]). The best way to study such a complex system as LN is to fix all parameters, except one, and to follow the change of crystal properties, if the chosen parameter is varied.

EPR spectra for different crystal compositions, but with the same chromium concentration, at the same temperature and with the same magnetic-field orientation with respect to the crystal axes, are compared in Figs. 6 and 7. Using a chromium concentration so small (0.02 wt. % in the melt) that the possibility of impurity aggregation is negligible, allows us to simplify the interpretation of the spectra. Four effects are clearly distinguishable when x_C increases: (1) all lines are getting more narrow; (2) additional satellite lines become more obviously seen; (3) the relative intensities I_n of

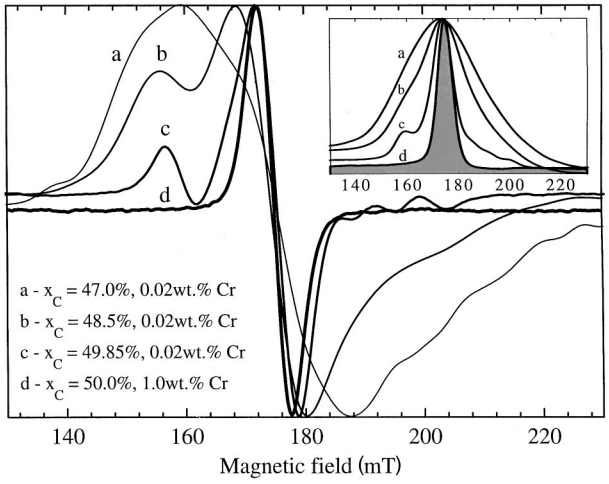

FIG. 7. First derivative of absorption line of Cr^{3+} central EPR transition for $\mathbf{B}\|\mathbf{x}$ for different x_C. Inset: original (integrated) absorption, $T = 4.2$ K.

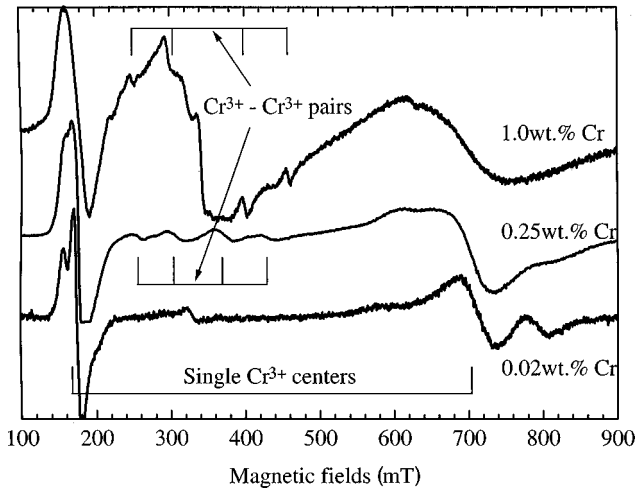

FIG. 8. Dependence of EPR spectra on chromium concentration for $x_C = 48.5\%$ (congruent composition). $\mathbf{B}\|\mathbf{x}$, $\nu = 9.4$ GHz, $T = 4.2$ K.

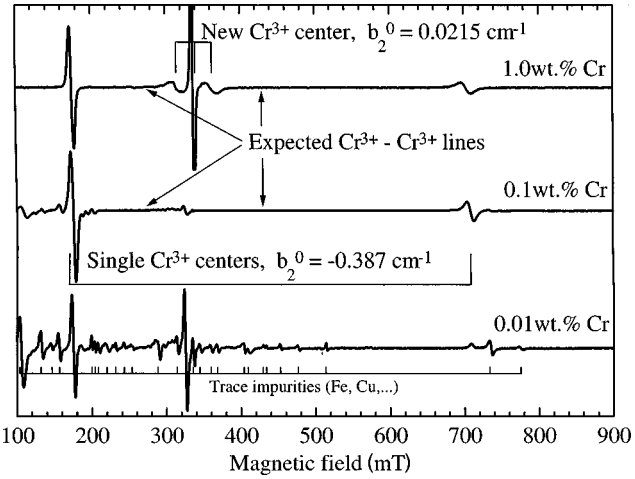

FIG. 9. Dependence of EPR spectra on chromium concentration for stoichiometric crystals. $\mathbf{B}\|\mathbf{x}$, $\nu = 9.4$ GHz, $T = 4.2$ K.

different lines (n is the line number) are changed; (4) some of the lines disappear. The first effect is a reliable indication of the improvement of the crystal perfection due to the decrease of the concentration of intrinsic defects. The differences between the areas under the original absorption lines in Fig. 7 [or integrated intensities in the case of the derivative lines $W_n \approx I_n(\Delta B_n)^2$, ΔB_n is the linewidth] show that the concentration of the centers responsible for the satellite lines is comparable to the concentration of the main axial center. It is also found that the change of the relative intensities I_n is not only related to the narrowing of the EPR lines, but also to the variation of the concentrations of different centers, if x_C is increased.

The comparison of the spectra of conventional congruent crystals (Figs. 7, 8) shows that they contain rather little information and are not very suitable for a detailed investigation, because their resonances are only poorly resolved. Since the lines from samples grown from a melt with Li excess are narrower, many additional satellite lines from such specimens were resolved close to the main lines. These spectra are able to give more information about chromium centers. In stoichiometric crystals this narrowing and the corresponding resolution are so tremendously high, that many noncontrolled trace impurities ($Cu^{2+}, Fe^{3+}, Mn^{2+}$) are now easily observed (see Fig. 9). However, the chromium satellite lines practically totally vanish in such stoichiometric samples (Figs 6 and 7). This disappearance of satellite EPR lines gives us a very useful tool to clarify the structure of many impurity defects and of Cr^{3+} in our particular case.

Figures 8 and 9 present the dependence of the EPR spectra on the chromium concentration in congruent and stoichiometric samples. The most significant observation is that additional EPR lines appear in congruent crystals at [Cr] $\geqslant 0.2$ wt. % in the melt. These lines were previously identified as originating from the state with $S = 2$ of low-symmetry exchange coupled Cr^{3+}-Cr^{3+} pairs.[15,29] However, such lines have not been registered in the samples with $x_C \approx 50\%$ even at [Cr] ≈ 1.0 wt.% in the melt.

ANGULAR DEPENDENCES OF CHROMIUM CENTERS IN NONSTOICHIOMETRIC AND STOICHIOMETRIC CRYSTALS

In order to determine the point-group symmetry and parameters of the spin Hamiltonians of the observed Cr centers an investigation of the full angular dependences of their EPR lines in **zx**, **xy**, and **yz** crystallographic planes (road map) was carried out. The road map of a nonstoichiometric crystal, but with an intentionally high $x_C = 49.5\%$, is given in Fig. 10. It should be noted that in this crystal also Fe^{3+} and Cu^{2+} trace impurities in rather low concentrations were detected; these ions are responsible for several lines with small intensities and well-known field positions: they were eliminated from Fig. 10 in order to avoid unnecessary complications of this rather detailed figure.

Chromium ions, depending on their charge state, have the following spin values: $Cr^{5+}(3d^1) - S = 1/2$, $Cr^{4+}(3d^2) - S = 1$, $Cr^{3+}(3d^3) - S = 3/2$, $Cr^{2+}(3d^4) - S = 2$ and $Cr^{+}(3d^5) - S = 5/2$. A detailed analysis of the observed spectra shows that all EPR lines (dots in Fig. 10) belong to Cr^{3+} ions with $S = 3/2$; there are no lines at these angular dependences, which could be related to other charge state or other defects. Most of the additional satellite lines are located near the lines of the main axial center and they have a similar angular behavior. Some of them never split for any orientation of the magnetic field and have no angular dependence in the **xy** plane. These lines belong to centers with C_3 point-group symmetry. Besides the main center, two such additional C_3 axial centers were found. All other lines, i.e., lines of C_1 centers, are split, if the magnetic field deviates from the **z** axis, and have a specific angular dependence in the **xy** plane. Six electrically nonequivalent low-symmetry centers were definitely identified. The spin-Hamiltonian parameters of all these centers, determined by fitting of the experimental angular dependences, are listed in Table II. Simulated angular dependences of the main axial and one low-symmetry center (Nos. 1 and 2 in Table II) are drawn in Fig. 10 as examples.

The values of the crystal-field parameters for all centers depend on the observation temperature. For example, the b_2^0 parameters of the main axial center changes from -0.41 cm^{-1} at room temperature to -0.386 cm^{-1} at liquid-helium

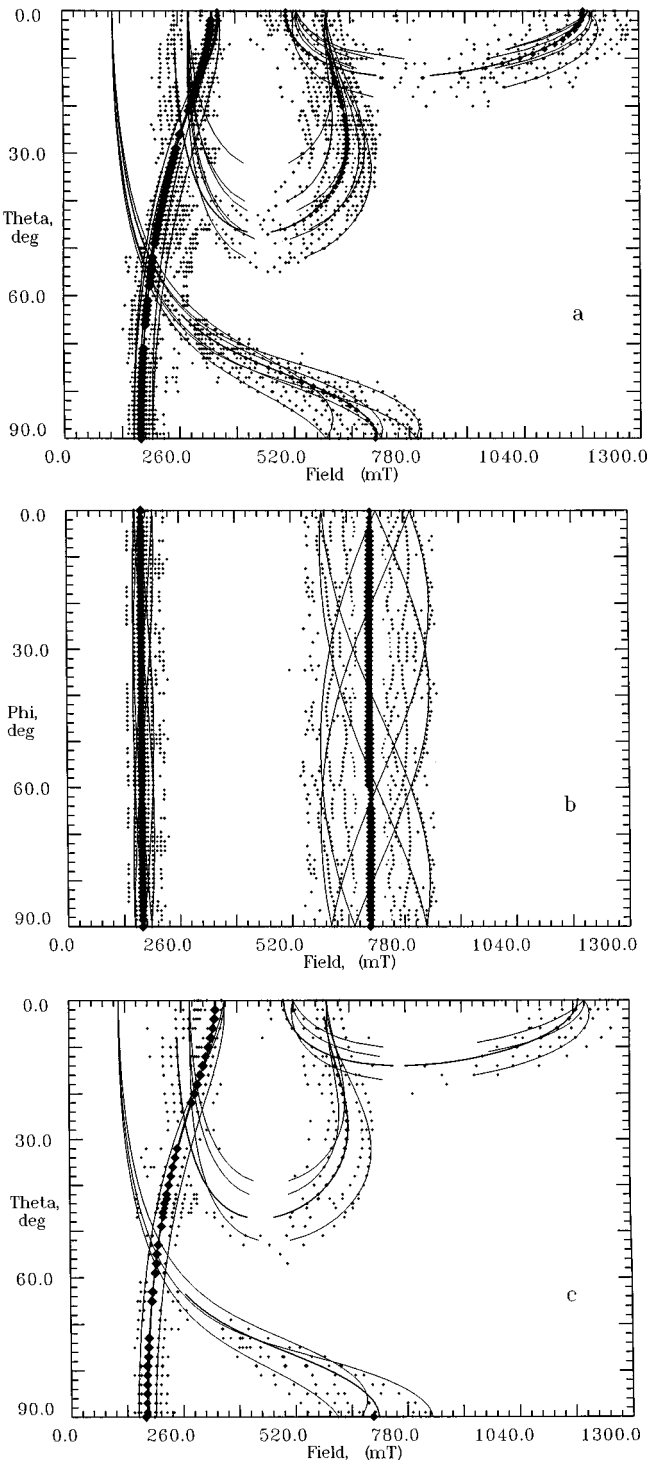

FIG. 10. Angular dependence of EPR lines for the LN:Cr crystal with $x_C = 49.5\%$. Symbol size is proportional to the intensity of observed EPR line. Calculated curves correspond to the main axial (thick) and one of the low-symmetry centers (No. 1 and No. 2 in the Table II). *a,b,c* are the **zx**, **xy**, and **zy** planes, $T = 4.2$ K.

temperature. This fact, the rather low resolution in congruent crystals and the treatment of the spectra by perturbation theory are the main reasons why other authors[1,2,4,14] have quoted somewhat different values. These circumstances should thus be taken into account if a comparison is made with data in other publications.

Fragments of the full experimental angular dependences (rotation of **B** only in the **xy** plane), as shown in Fig. 11, convincingly demonstrate differences between EPR spectra of nonstoichiometric and stoichiometric crystals. The two EPR lines without angular dependence, which are observed in the spectra of stoichiometric crystals, belong to the main axial Cr^{3+} center and to the axial center of Fe^{3+} ions (the latter have more intensive signals). It can be seen in Fig. 11 that the lines of all axial and low-symmetry satellite chromium centers completely disappear in a crystal with $x_C = 50\%$.

However, in all other LN crystals of congruent and nonstoichiometric compositions these satellite lines are present. Taking into account all considered data, we can conclude that (1) all satellite centers have the same nature; (2) they are some associations of Cr^{3+} and intrinsic nonstoichiometric defects; (3) in the range of concentration 0.002–0.2 wt. % chromium ions prefer only one lattice site.

OPTICAL ABSORPTION AND LUMINESCENCE

Due to the high sensitivity to the variation of crystal composition and to the presence of background impurities even in the very small concentration of less than 10^{-2} wt. %, spectra of crystals grown by somewhat different methods and from various starting materials are very often not identical. To facilitate the search for the correlation of the optical absorption and luminescence spectra to the centers identified by EPR, we studied such spectra with the same sets of LN crystals, which had been investigated by EPR.

In the optical absorption spectra (Fig. 12) there are no pronounced changes in the position of the known bands[3,7] of Cr^{3+}, if x_C increases from congruent to stoichiometric composition; this is valid at least for chromium doping up to 0.1 wt. % in the melt. However, some other effects can be clearly identified for increasing x_C: (1) a blueshift of the absorption edge, which reflects the improvement of the crystal lattice by the elimination of nonstoichiometric defects;[57,58] (2) some narrowing of the Cr^{3+} absorption lines (similar to that observed in Ref. 21); (3) a considerable reduction of chromium absorption: although the chromium concentration in the melt for congruent crystals was five times lower, the observed absorption coefficient at 660 nm for such a congruent sample is 14 times larger than for the stoichiometric one. The latter feature can be explained by a decrease of the coefficient of the Cr^{3+} incorporation into the crystals, if the Li content x_C rises and the specimen becomes more stoichiometric. This is in good agreement with our EPR data. Since absorption bands of the dominating $^4A_2 \leftrightarrow {}^4T_2, {}^4T_1$ transitions are rather broad, it is difficult to separate the contributions of different centers from each other. The weak, but notably more narrow, zero-phonon *R* lines, which correspond to $^4A_2 \leftrightarrow {}^2E$ transitions, could be more informative for our purpose. Since they are also not very intensive in the absorption spectra taken at room temperature, these lines were reanalyzed in luminescence spectra measured at $T = 10$ K.

A single Cr^{3+} center usually gives only one doublet of *R* lines. More than two lines were previously registered for congruent crystals. They were related to different centers.[19] In the fragments of luminescence spectra measured with our series of LN crystals with different x_C (Fig. 13, Ref. 59) it is possible to distinguish even more lines. They can especially

TABLE II. Characteristics of Cr^{3+} centers in $LiNbO_3$ at 4.2 K (parameters of crystal field are given in cm^{-1}). The arrangement of the centers approximately corresponds to the relative intensities of their EPR lines in LN crystals with $x_C = 49.85\%$.

Center No.	Symmetry	g	b_2^0	$\pm b_2^1$	c_2^1	b_2^2	$\pm c_2^2$	Zero-field splitting $2\|\Delta\|$	Suggested model, shell number (equivalent sites)
1	$\mathbf{C}_3$, axial	1.972	−0.3865					0.773	Cr_{Li}, main center, (1)
2	$\mathbf{C}_1$	1.97	−0.4010	0.094	−0.124	0.080	0.069	0.814	$Cr_{Li}+v_{Nb}$, 6 (3)
3	$\mathbf{C}_1$	1.97	−0.3845	0.052	0.100	−0.064	0.050	0.777	$Cr_{Li}+v_{Nb}$, 9 (6)
4	$\mathbf{C}_1$	1.97	−0.3475	0.088	0.075	0.036	0.062	0.703	$Cr_{Li}+v_{Nb}$, 7 (3)
5	$\mathbf{C}_1$	1.97	−0.4235	0.076	−0.159	0.0635	0.020	0.856	$Cr_{Li}+v_{Nb}$, 5 (6)
6	$\mathbf{C}_3$, axial	1.97	−0.3710					0.742	$Cr_{Li}+v_{Nb}$, 1 or 4 (1)
7	$\mathbf{C}_3$, axial	1.97	−0.4220					0.844	$Cr_{Li}+v_{Nb}$, 4 or 1 (1)
8	$\mathbf{C}_1$	1.97	−0.4300	0.010	0.070	0.047	0.105	0.871	$Cr_{Li}+v_{Nb}$, 2 (3)
9	$\mathbf{C}_1$	1.97	−0.4070	0.135	−0.137	−0.120	0.050	0.835	$Cr_{Li}+v_{Nb}$, 3 (3)

obviously be seen in the spectrum of a LN crystal with $x_C = 49.85\%$, where luminescence lines are already noticeably more narrow and better resolved than in congruent samples. However, whole groups of lines in the surrounding of L_1, L_2, which are present in the congruent crystals, are absent in the spectrum of LN with $x_C = 50\%$. This means that those lines do not belong to the main axial chromium center, and they thus should be assigned to the satellite centers.

DETERMINATION OF CHROMIUM POSITION

Attempts to determine impurity positions by indirect methods often gave contradicting information. Many of the direct methods are not applicable to the solution of this task in the LN:Cr system: Mössbauer spectroscopy[60] demands the presence of special nuclei; channeling investigations (Rutherford backscattering spectrometry[61]) are more successful in the case of heavy, many-electron ions.

In pioneer articles[1–3] it was assumed that chromium occupies the Nb site. Later, however, on the basis of EPR data,[14] it was concluded that the main axial chromium center with $b_2^0 \approx -0.39\,cm^{-1}$ has to be attributed to Cr on a Li site. In the measurements[15] of electron nuclear double resonance (ENDOR) of this Cr center in LN crystals, grown from congruent and stoichiometric melts, parameters of hyperfine (49.3 MHz) and quadrupole (−0.37 MHz) interactions for ^{53}Cr were determined. The rather strong value of the observed quadrupole interaction was in agreement with the Cr_{Li}^{3+} assignment.

Another chromium center with $b_2^0 \approx 0$ appears in LN codoped with 6 mol. % of Mg. ENDOR investigations of this center[12,62] showed that the observed hyperfine interactions with several shells of surrounding Li nuclei can be explained by assuming that chromium occupies the Nb site. This was supported by the small value of $b_2^0 (\leqslant 0.01\,cm^{-1})$ and quadrupole interaction (0.1 MHz), more likely to occur for the Nb than for the Li site, and by comparison with the corresponding parameters[14,15] of the chromium center in LN not codoped with Mg. However, in making a comparison of both types of Cr centers one has to consider: (a) LN without Mg and LN heavily doped with Mg are very different crystals with respect to both the intrinsic and extrinsic defect subsystems; (b) the disappearance of chromium centers with $|b_2^0| \approx 0.4\,cm^{-1}$ in LN:Mg could be explained, for instance, by the change of the charge compensator in the nearest neighborhood instead of another chromium position. Therefore, it would be rather risky, to ascribe the main axial center to the Li site, solely on the basis of ENDOR data for the center with $b_2^0 \approx 0$ in LN:Mg,[19,27] without detailed investigation of hyperfine interactions of this main center with its surroundings.

Results obtained by an extended x-ray-absorption fine-structure analysis were in favor of Li substitution,[18] however these measurements were made for LN crystals with a high dopant level of about 5 mol. %, for which clustering and occupation of both Li and Nb position becomes very probable. The best fit of the data of particle induced x-ray emission combined with channeling[28] was obtained assuming 60% of the Cr occupying regular Li sites and 40% occupying regular Nb sites. However, this method is not sensitive to the

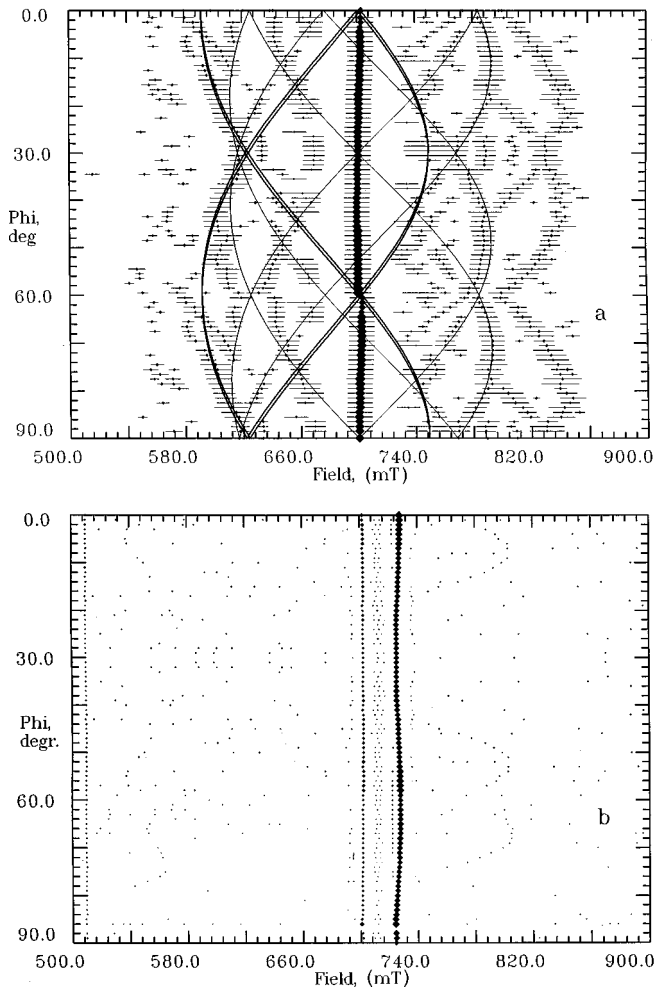

FIG. 11. Fragments of angular dependences of EPR lines in the **xy** plane in nonstoichiometric (a) and stoichiometric (b) LN:Cr crystals. $v = 9.4$ GHz, $T = 4.2$ K. Solid lines: calculated angular dependences of two low-symmetry centers (Nos. 3 and 4 in the Table II).

charge state of the impurity and does not distinguish C_3 and C_1 centers.

In order to have a direct evidence for the Cr^{3+} position, we carried out a full ENDOR investigation for the main axial

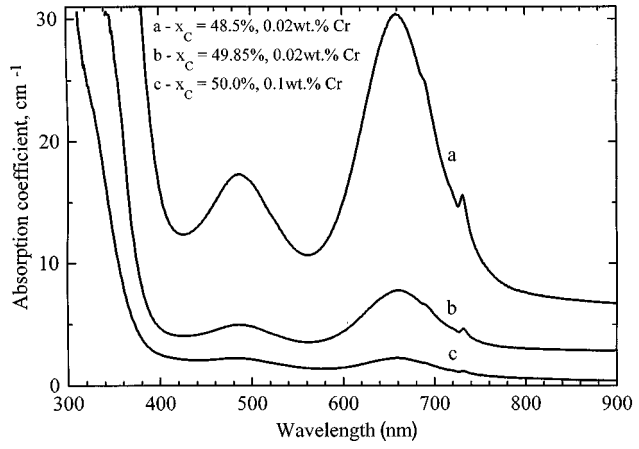

FIG. 12. Optical absorption spectra in congruent and stoichiometric LN:Cr.

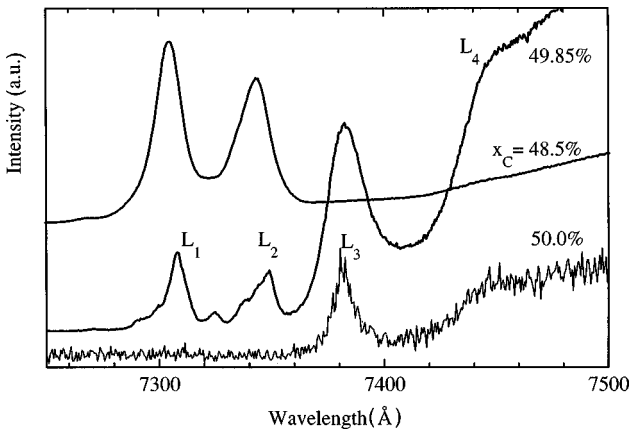

FIG. 13. Fragments of luminescence spectra in congruent, nearly stoichiometrics and stoichiometric LN:Cr (after Ref. 59). Excitation wavelength 514.5 nm.

center in LN.[63] We found that in our case the hyperfine interactions with Nb nuclei are much stronger than with the Li nuclei. This means that Cr^{3+} has a Nb nuclei in its first coordination shell and thus replaces Li^{+}. This conclusion is supported by further observations.[63]

PROPOSED MODELS OF CHROMIUM CENTERS AND INTERPRETATION OF THE RESULTS

Due to the similar behavior of all satellite centers under variation of the Cr content and of x_C one common idea should be used for the explanation of the presence of different axial and low-symmetry chromium centers.

On the basis of all available to us data, we found the following explanation of all results, which is free of contradictions. The main axial center is Cr^{3+} located at a site with C_3 symmetry without any other defect in its nearest neighborhood (distant charge compensation). All satellite axial or low-symmetry centers have some intrinsic defects in their surroundings (local charge compensation). For a small Cr^{3+} content a lowering of the concentration of nonstoichiometric defects leads to a narrowing of the EPR lines, to more symmetrical line shapes and to a decrease of the line intensity of the forbidden transitions. Due to the lack of local and distant charge compensators in stoichiometric crystals all satellite centers disappear and the concentration of the main centers decreases.

The larger the distance of the compensating defect from Cr^{3+} the less the crystal-field parameters of this center deviate from those of the main axial center, the less is the splitting between its lines and main center lines, and the more difficult it is to resolve the structure of the overlapping lines. For a random distribution of distant intrinsic defects most of them are located away from the C_3 axis. This leads to random variations of the crystal-field parameters b_k^q with $q \neq 0$ and to the specific asymmetry of the EPR lines at $\mathbf{B} \| \mathbf{z}$ in nonstoichiometric crystals. The close similarity of the simulated line shapes and the observable EPR line (Fig. 14) supports our hypothesis about the origin of the line asymmetry.

Let us discuss the nature of the defects, which produce the family of axial and low-symmetry centers. The unintended trace impurities can be excluded from the consideration, be-

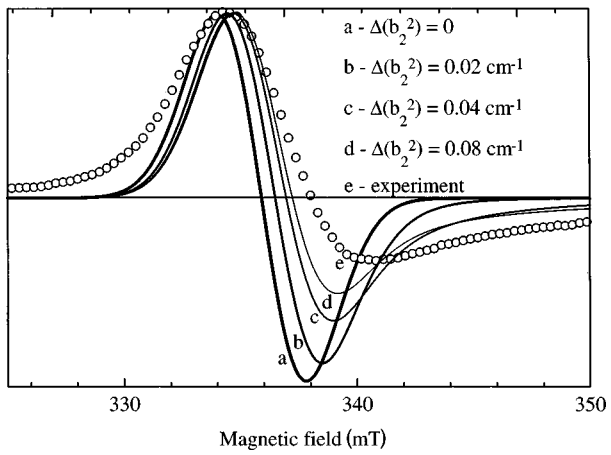

FIG. 14. Simulated dependence of line shape on random distribution of crystal-field parameter b_2^2 at $\mathbf{B}\|\mathbf{z}$. Δ is the width of the random distribution function. (a)–(d) are the calculations for the $1/2 \leftrightarrow -1/2$ EPR transition of the center with $g=1.97$, $b_2^0=-0.387$, and for $\nu=9.4$ GHz. (e) is the experimental line including overlapping lines of all axial and low-symmetry chromium centers; $x_C=48.5\%$, 0.02 wt. % Cr, $T=4.2$ K.

cause their content usually does not exceed $0.00X$ mol. %, whereas the generally used chromium concentrations in our samples were much higher. The selection of possible intrinsic defects can also be limited to point defects, such as vacancies of Li, Nb, O, interstitial ions and antisite defects Nb_{Li}, Li_{Nb}. Agglomerations of two or more intrinsic defects around a chromium ion can be taken into account additionally; these, however are less probable, if the defects are uniformly or randomly distributed. Complexes of Cr^{3+} and an oxygen vacancy or other defects in the oxygen sublattice as well as the occupation of the tetrahedral vacancy by chromium have to be rejected, because they have C_1 symmetry only, but axial satellite centers were also identified in our experiments. Oxygen interstitial ions could lead to C_3 and C_1 centers; such a hypothesis, however, cannot directly explain the disappearing of EPR lines if x_C increases. Moreover, the lines of all Cr centers are not very sensitive to strong reduction-oxidation annealing treatments. This would take place if centers were present involving interstitial oxygen or oxygen vacancies.

Furthermore the probability that LN crystals with a Li deficit have a high concentration of Li interstitial ions or Li_{Nb} is rather small. Therefore, only antisite Nb_{Li} for Cr_{Nb} substitution and lithium or niobium vacancies for the case of Cr_{Li} have to be considered seriously. Our determination of Cr_{Li} substitution with the help of ENDOR (Ref. 63) allows us to discard the possibility of charge compensation by Nb_{Li} for the main chromium center in LN (such a possibility nevertheless remains for other dopants and centers).

On the basis of $Cr_{Li^+}^{3+}-2v_{Li^+}$ models it is difficult to explain the number of observed chromium centers of C_3 and C_1 types and the values of their spin-Hamiltonian parameters. If we suppose that three clearly resolved axial centers with zero-field splitting 2Δ equal to 0.742, 0.773 (main center) and 0.844 cm^{-1} consist of $Cr_{Li^+}^{3+}$ and one or two lithium vacancies at distance 6.93 Å, the low-symmetry centers associated with the vacancies at much shorter distances ($r=3.76$ Å, four centers and $r=5.15$ Å, 12 centers) should also be well resolved and should have 2Δ values much smaller than 0.742 cm^{-1} or much larger than 0.844 cm^{-1}. However, the smallest and the largest splitting of energy levels for the observed C_1 centers (0.7 and 0.86 cm^{-1}, see Table II) are approximately equal to those of the axial centers. This is thus in contradiction to the assumption that $Cr_{Li^+}^{3+}$ is compensated by v_{Li}. The number of detected centers is also less than predicted for this model, but it is possible to imagine that not all of them are resolved. This argument cannot be easily discarded, because the narrowest lines even for the sample with $x_C=49.85\%$ have widths of about 5 mT ≈ 0.005 cm^{-1}.

Models with niobium vacancies give a more logical and reliable explanation of the existence of the centers with the obtained parameters. All satellite centers are Cr_{Li} centers with v_{Nb} in the first-ninth niobium shells (Fig. 2). The main chromium center most probably has no v_{Nb} in its neighborhood, however, the presence of v_{Nb} in the first niobium shell on the z axis should be considered as a possible alternative (unfortunately, vacancies cannot be detected directly by EPR or ENDOR). The proposed correspondence of the center parameters and their models are indicated in Table II.

The observation of only low-symmetry (but not axial) exchange coupled chromium pairs in nonstoichiometric crystals at a comparatively low Cr concentration and their disappearance in stoichiometric samples becomes also understandable in the frame of the chosen idea: these pairs are C_1 complexes formed from one v_{Nb} and two Cr_{Li}, which are situated in the nearest Li sites. Four lithium vacancies instead of one v_{Nb} would be necessary to ''glue'' such a $Cr_{Li^+}^{3+}$-$Cr_{Li^+}^{3+}$ pair. Self-compensated $Cr_{Li^+}^{3+}$-$Cr_{Nb^{5+}}^{3+}$ pairs should be independent of the crystal stoichiometry or should react just oppositely to its changes, i.e., due to self-compensation the concentration of such pairs should not decrease with rising x_C.

Considering the data available at present, we cannot exclude the possibility of combined local and intermediate compensation of Me_{Li}^{3+} by several kinds of vacancies. For example, by one v_{Nb} and one oxygen vacancy or by v_{Li} in the first Li shell and by v_{Nb} in one of Nb shells, where v_{Nb} is shared by several impurity ions. The presence of both cation vacancies in nonstoichiometric LN was used for the interpretation of recent results of x-ray analysis[53] (split model of intrinsic defects) and high resolution electron microscopy[56] (Nb_2O_5 molecules incorporated into $LiNbO_3$ or a complex of $2Nb_{Li}+2Nb_v+3v_{Li}+3v_{Nb}$ replacing a regular sequence of lattice ions). The advantage of the scheme suggested above, Cr_{Li}^{3+} compensation by v_{Nb}, is that it is sufficient to explain all experimental facts on the basis of minimal number of assumed defects. It especially avoids the inconsistencies connected with the v_{Li} model. It is open, however, whether really a more complicated compensation mechanism occurs.

It could be argued that the presence of niobium vacancies is energetically unfavorable. However, we expect that the total energy for the creation of complexes consisting of two or more defects (v_{Nb} and Nb_{Li}, v_{Nb} and Nb_v, the complexes mentioned above) can be less than the energy for the creation of isolated v_{Nb} only, like in the case of Frenkel or Schottky defects in alkali halides. Therefore, the existence of v_{Nb} as

one of the elements of the nonstoichiometric defect structure cannot simply be rejected.

CONCLUSIONS AND DISCUSSION

The reported detailed analysis and classification of possible complexes of impurity and intrinsic defects allow us to understand the main features of the observed spectra. Besides the main axial Cr^{3+} center, eight satellite chromium centers are definitely resolved. The determined parameters of their spin Hamiltonians give a reliable starting point for further investigations and theoretical calculations. The existence of a family of chromium centers (three axial and six low-symmetry centers) was explained on the basis of one common hypothesis about charge compensation by intrinsic defects.

Summarizing all our results the following conclusions can be made:

(i) In all LN crystals of congruent and nonstoichiometric composition further chromium centers have been observed in addition to the main axial center. It was found that the crystals with high $x_C \approx 49.5$–$49.85\,\%$ are the most suitable ones for a detailed investigation of such additional centers. Their spectra are much more informative, because of the tremendous narrowing of the resonance lines in comparison with those in congruent crystals.

(ii) The widths of the Cr EPR lines and the intensity ratios of the forbidden and allowed transitions can be used as probes of crystal perfection (as reported for the EPR lines of iron as a background impurity[42,44]).

(iii) The satellite centers are formed by pairs of defects, such as Cr_{Li}-v_{Nb} and are influenced by the corresponding distortion of the LN lattice around these defects. Two v_{Nb} are charge compensators for five Cr_{Li}.

(iv) A family of satellite chromium centers exists due to the different relative locations of the impurity ion and its charge compensator: v_{Nb} in these cases would then be located in the first, second, third, and the following neighboring Nb shells.

(v) The satellite centers have much larger values of electrical dipole moments than isolated Cr^{3+} because of the excess charges of both $Cr_{Li^+}^{3+}$ and $v_{Nb^{5+}}$ defects; these dipole moments are expected to have a strong interaction with the static and optical electric fields.

(vi) With the help of EPR, experimental evidence was found that one of the main nonstoichiometric defects in LN is related to v_{Nb}. Together with the existence of Nb_{Li} (also detected by EPR previously[64–67]) it gives an essential argument for the development of intrinsic defect models.

Since the relative concentrations of additional satellite centers are comparable with the concentration of the main center, both kinds of centers generally are equally responsible for many of the properties of nonstoichiometric LN crystals, and they should both be taken into consideration, especially in congruent crystals.

The existence of several electrically nonequivalent centers is not a feature specific for only chromium ions in LN. Two or more different centers were observed for Nd^{3+},[2,68,69] Fe^{3+},[14,70] Er^{3+},[71] Yb^{3+}.[72] It is quite clear now that most of them are complexes of the dopant ion–intrinsic defect or dopant ion–unintended background impurity.

The presence of nonstoichiometric defects is one of the reasons why LN tolerates a strong incorporation of dopants nonisovalent to Li^+ and Nb^{5+}. As long as the impurity concentration [Me] is smaller than $\delta x_C = |50\% - x_C|$, the number of intrinsic defects is large enough to compensate the corresponding charge excess. However, for stoichiometric or nearly stoichiometric samples with high impurity concentrations (when $[\mathrm{Me}] > \delta x_C$) and with the lack of charge compensators a decrease of the distribution coefficient of impurities is observed in comparison with congruent material. A further increase of the $[\mathrm{Me}]/\delta x_C$ ratio up to $[\mathrm{Me}] \gg \delta x_C$ can result in a change of the charge compensation mechanism; this can reveal itself in the appearance of new impurity centers [as in the case of Fe^{3+} (Ref. 73)], i.e., self-compensated impurity-impurity complexes. The increase of the dopant concentration in the melt can, however, also lead to the inverse tendency: a lowering of x_C or even a reconstruction of the nearest neighborhood of the impurity, because the formation of intrinsic defects might be an energetically favorable compensation mechanism, depending on the type of dopant ion. This strong interrelation between the subsystems of extrinsic and intrinsic defects[74] is one of the most important features of LN. Only a combined study of both subsystems can lead to the successful tailoring of the properties of LN for possible new applications and for its optimization for already existing utilization.

It is interesting to note that changes of some characteristics of LN (for instance, its electro-optic coefficients[75,76]) depend in a parallel way on the increase of the chromium concentration and of x_C (at least, for [Cr] less than about 0.1 wt. %). This means that doping LN with Cr leads to a kind of partial healing of nonstoichiometric defects. This happens because Cr, entering from the melt to the LN lattice, occupies the Li position and decreases the amount of Nb ions in two ways: by elimination of Nb_{Li} antisites and by the possible creation of v_{Nb}. Both processes effectively result in an increase of the Li/Nb ratio. Because of this obviously strong relation between extrinsic and intrinsic defects, it would be logical to expect a certain threshold or nonmonotonic dependence of the properties of LN on the change of the Cr concentration [similar to LN with other trivalent impurities, such as In,[77,78] Sc (Ref. 79)].

A strong broadening of the spectral lines of LN crystals, occurring if crystals are heavily doped with Mg (or other impurities suppressing optical damage), decreases the resolution of the various spectroscopic techniques. However, the spectral resolution is very important for the study of such crystals, where the structure and behavior of the impurity defects are expected to be even more complicated than in nonstoichiometric samples without damage resistant impurities, since they depend in this case on three variables: δx_C, [Me], and [Mg]. These difficulties can lead to doubtful judgments about defect structures. The use of stoichiometric crystals with $\delta x_C = 0$ presents many advantages for the investigation of impurity centers; it leads to high resolution and sensitivity, facilitates the analysis of the spectra, and simplifies the interpretation of the data.

ACKNOWLEDGMENTS

In its various stages this work has been partly supported by grants from INTAS, BMBF, ESF, DFG (in the frame of SFB 225). It was carried out in cooperation with many scientists. We are very grateful to all members of the Magnetic Resonance Spectroscopy Group at the University of Osnabrueck, to Dr. H. Hesse for fruitful discussions and to E. Bondarenko for accurate and patient crystal preparation. Dr. A. Hofstaetter and Professor A. Scharmann (University of Giessen) kindly provided the opportunity to perform a part of ENDOR measurements of the main Cr center.

*Electronic address: gmalovic@mail.rz.uni-osnabrueck.de

[1] G. Burns, D. F. O'Kane, and R. S. Title, Phys. Rev. **147**, 314 (1967).
[2] N. F. Evlanova, L. S. Kornienko, L. N. Rashkovich, and A. O. Rybaltovskii, Sov. Phys. JETP **26**, 1090 (1968).
[3] A. M. Glass, J. Chem. Phys. **50**, 1501 (1969).
[4] D. J. Rexford, Y. M. Kim, and H. S. Story, J. Chem. Phys. **52**, 860 (1970).
[5] D. J. Rexford and Y. M. Kim, J. Chem. Phys. **57**, 3094 (1972).
[6] A. P. Skvortsov, V. A. Trepakov, and L. Jastrabik, Phys. Solid State **39**, 1930 (1997); J. Lumin. **72–74**, 716 (1997).
[7] A. M. Glass and D. H. Auston, Opt. Commun. **5**, 45 (1972).
[8] M. G. Clark, F. G. Disalvo, A. M. Glas, and G. E. Peterson, J. Chem. Phys. **59**, 6209 (1973).
[9] F. M. Michel-Calendini, P. Moretti, and H. Chermette, Cryst. Lattice Defects Amorphous Mater. **15**, 65 (1987).
[10] L. Kovacs and K. Polgar, Cryst. Res. Technol. **21**, K101 (1986).
[11] A. Martin, F. J. Lopez, and F. Agullo-Lopez, J. Phys.: Condens. Matter **4**, 847 (1992).
[12] G. Corradi, H. Soethe, J.-M. Spaeth, and K. Polgar, J. Phys.: Condens. Matter **3**, 1901 (1991).
[13] M. G. Zhao and Y. Lei, J. Phys.: Condens. Matter **9**, 529 (1997).
[14] G. I. Malovichko, V. G. Grachev, and S. N. Lukin, Sov. Phys. Solid State **28**, 553 (1986).
[15] V. G. Grachev, G. I. Malovichko, and V. V. Troitskii, Sov. Phys. Solid State **29**, 349 (1987).
[16] S. H. Choh, H. T. Kim, H. K. Choh, C. S. Han, D. Choi, and J. N. Kim, Bull. Magn. Reson. **11**, 371 (1989).
[17] T. H. Yeom, Y. M. Chang, C. Rudowicz, and S. H. Choh, Solid State Commun. **87**, 245 (1993).
[18] G. Corradi, A. V. Chadwick, A. R. West, K. Cruickshank, and M. Paul, Radiat. Eff. Defects Solids **134**, 219 (1995).
[19] P. I. Macfarlane, K. Holliday, J. F. H. Nicholls, and B. Henderson, J. Phys.: Condens. Matter **7**, 9643 (1995).
[20] P. I. Macfarlane, K. Holliday, and B. Henderson, Chem. Phys. Lett. **252**, 311 (1996).
[21] C. Fischer, S. Kapphan, Xi-Qi Feng, and Ning Cheng, Radiat. Eff. Defects Solids **135**, 199 (1995).
[22] J. Diaz-Garo, J. Garcia Sole, D. Bravo, J. A. Sanz-Garcia, F. J. Lopez, and F. H. Jaque, Phys. Rev. B **54**, 13 042 (1996).
[23] J. N. Kim and H. L. Park, J. Korean Phys. Soc. **15**, 12 (1982).
[24] V. G. Grachev and G. I. Malovichko, Sov. Phys. Solid State **27**, 1678 (1985).
[25] M. D. Glinchuk, G. I. Malovichko, I. P. Bykov, and V. G. Grachev, Ferroelectrics **92**, 83 (1989).
[26] J. Garcia Sole, A. Monteil, G. Boulon, E. Camarillo, J. O. Tocho, I. Vergara, and F. Jaque, J. Phys. IV , C7-403 (1991).
[27] K. Holliday and P. Macfarlane, J. Phys.: Condens. Matter **9**, 6475 (1997).
[28] A. Kling, J. C. Soares, M. F. da Silva, J. A. Sanz-Garsia, E. Dieguez, and F. Agullo-Lopez, Nucl. Instrum. Methods Phys. Res. B **136-138**, 426 (1998).
[29] V. Grachev, G. Malovichko, and O. Schirmer, Ferroelectrics **185**, 5 (1996).
[30] Weiyi Jia, H. Liu, R. Knutson, and W. M. Yen, Phys. Rev. B **41**, 10 906 (1990).
[31] Weiyi Jia, H. Liu, S. Jaffe, W. M. Yen, and B. Denker, Phys. Rev. B **43**, 5234 (1991).
[32] G. G. Siu and Z. MinGuang, Phys. Rev. B **43**, 13575 (1991).
[33] E. Camarillo, J. Garcia Sole, F. Cusso, F. Agullo-Lopez, J. A. Sanz-Garcia, T. P. J. Han, F. H. Jaque, and B. Henderson, Chem. Phys. Lett. **185**, 505 (1991).
[34] E. Camarillo, J. Tocho, F. Vergara, E. Diegues, J. Garcia Sole, and F. H. Jaque, Phys. Rev. B **45**, 9 (1992).
[35] Y. M. Chang, T. H. Yeom, Y. Y. Yeung, and Ch. Rudowicz, J. Phys.: Condens. Matter **5**, 6221 (1993).
[36] J. F. H. Nicholls, T. P. J. Han, B. Henderson, and F. Jaque, Chem. Phys. Lett. **202**, 6 (1993).
[37] F. Jaque, J. Garcia Sole, E. Camarillo, F. J. Lopez, H. Murrieta, J. Hernandez, Phys. Rev. B **47**, 5432 (1993).
[38] B. Macalic, J. E. Bausa, J. Garcia Sole, and F. H. Jaque, Appl. Phys. Lett. **62**, 16 (1993).
[39] P. F. Bordui, R. G. Norwood, C. D. Bird, and G. D. Calvert, J. Cryst. Growth **113**, 61 (1991).
[40] K. Kitamura, Y. Furukawa, and N. Iyi, Ferroelectrics **202**, 21 (1997).
[41] G. I. Malovichko, V. G. Grachev, L. P. Yurchenko, V. Ya. Proshko, E. P. Kokanyan, and V. T. Gabrielyan, Phys. Status Solidi A **133**, K29 (1992).
[42] G. I. Malovichko, V. G. Grachev, E. P. Kokanyan, O. F. Schirmer, K. Betzler, B. Gather, F. Jermann, S. Klauer, U. Schlarb, and M. Wöhlecke, Appl. Phys. A: Solids Surf. **A56**, 103 (1993).
[43] K. Polgar, A. Peter, L. Kovacs, G. Corradi, and Zs. Szaller, J. Cryst. Growth **177**, 211 (1997).
[44] G. I. Malovichko, V. G. Grachev, and O. F. Schirmer, Solid State Commun. **89**, 195 (1994).
[45] V. G. Grachev, 1992–1998. All details and light version to download can be found on home page http://www.physik.uni-osnabrueck.de/resonanz/Grachev.
[46] S. C. Abrahams, J. M. Reddy, and J. L. Bernstein, J. Phys. Chem. Solids **27**, 997 (1966).
[47] S. C. Abrahams, W. C. Hamilton, and J. M. Reddy, J. Phys. Chem. Solids **27**, 1013 (1966).
[48] S. C. Abrahams, H. J. Levinstein, and J. M. Reddy, J. Phys. Chem. Solids **27**, 1019 (1966).
[49] A. Räuber, in *Current Topics in Material Sciences*, edited by E. Kaldis (North-Holland, Amsterdam, 1978), Vol. XX, p. 481.
[50] N. Iyi, K. Kitamura, Izumi F. J. K. Yamamoto, T. Hayashi, H. Asano, and S. Kimura, J. Solid State Chem. **101**, 340 (1992).
[51] S. A. Altshuler, B. M. Kozirev, *Electron Paramagnetic Resonance in Compounds of Transition Elements* (Wiley, New York, 1974).
[52] P. Lerner, C. Legras, and J. P. Dumas, J. Cryst. Growth **3/4**, 231 (1968).

[53] N. Zotov, H. Boysen, F. Frey, T. Metzger, and E. Born, J. Phys. Chem. Solids **55**, 145 (1994).
[54] S. C. Abrahams and P. Marsh, Acta Crystallogr., Sect. B: Struct. Sci. **42**, 61 (1986).
[55] G. E. Peterson and A. Carnevale, J. Chem. Phys. **56**, 4648 (1972).
[56] Ch. Leroux, G. Nihoul, G. Malovichko, V. Grachev, and Cl. Boulesteix, J. Phys. Chem. Solids **59**, 311 (1998).
[57] D. Redfield and W. J. Burke, J. Appl. Phys. **45**, 4566 (1971).
[58] I. Földvari, K. Polgar, and A. Mecseki, Acta Phys. Hung. **55**, 321 (1984).
[59] F. Lhomme, P. Bourson, M. D. Fontana, G. Malovichko, M. Aillerie, and E. Kokanyan, J. Phys.: Condens. Matter **10**, 1137 (1998).
[60] R. Vianden, in *Insulating Materials for Optoelectronics. New Developments*, edited by F. Agullo-Lopez (World Scientific, Singapore, 1995), p. 125.
[61] A. Kling, J. C. Soares, and M. F. da Silva, in *Insulating Materials for Optoelectronics. New Developments* (Ref. 60), p. 175.
[62] G. Corradi, H. Söthe, J.-M. Spaeth, and K. Polgar, Ferroelectrics **125**, 295 (1992).
[63] G. Malovichko, V. Grachev, A. Hofstaetter, A. Scharmann, and O. Schirmer (unpublished).
[64] O. F. Schirmer and D. Linde, Appl. Phys. Lett. **33**, 35 (1978).
[65] H. Müller and O. F. Schirmer, Ferroelectrics **125**, 319 (1992).
[66] B. Faust, H. Müller, and O. F. Schirmer, Ferroelectrics **152**, 297 (1994).
[67] O. F. Schirmer, O. Thiemann, and M. Wöhlecke, J. Phys. Chem. Solids **52**, 185 (1991).
[68] A. Lorenzo, H. Loro, J. E. M. Santiuste, M. C. Terrile, G. Boulon, L. E. Bausa, and J. G. Sole, Opt. Mater. **8**, 55 (1997).
[69] F. Henecker, A. Hofstaetter, A. Scharmann, G. I. Malovichko, V. G. Grachev, and E. P. Kokanyan (unpublished).
[70] I. W. Park, S. H. Choh, K. J. Song, T. H. Yeom, and C. Rudowicz, J. Korean Phys. Soc. **26**, 168 (1993).
[71] T. Nolte, T. Pawlik, and J.-M. Spaeth, Solid State Commun. **104**, 535 (1997).
[72] G. Malovichko, V. Grachev, E. Kokanyan, and O. Schirmer (unpublished).
[73] G. I. Malovichko, V. G. Grachev, O. F. Schirmer, and B. Faust, J. Phys.: Condens. Matter **5**, 3971 (1993).
[74] G. Malovichko, V. Grachev, and O. Schirmer, in *Materiaux et Composants Piezo-Pyro-Ferro-Electriques*, Journees D'Etudes, Limoges, 19, 20 March 1996 (see Limoges, 1996).
[75] K. Chah, M. Aillerie, M. D. Fontana, G. I. Malovichko, and E. Kokanyan, Ferroelectrics **155**, 13(963) (1996).
[76] K. Chah, M. Aillerie, M. D. Fontana, G. I. Malovichko, K. Betzler, and E. Kokanyan, Opt. Commun. **136**, 231 (1997).
[77] T. Volk, N. Rubinina, and V. Pryalkin, Opt. Lett. **15**, 996 (1990).
[78] T. Volk, M. Wöhlecke, N. Rubinina, N. V. Razumovski, F. Jermann, C. Fischer, and R. Böwer, Appl. Phys. A: Mater. Sci. Process. **60A**, 217 (1995).
[79] J. K. Yamamoto, K. Kitamura, N. Iyi, S. Kimura, Y. Furukawa, and M. Sato, Appl. Phys. Lett. **61**, 2156 (1992).